Heliyon 10 (2024) e36074

Contents lists available at ScienceDirect

Heliyon

journal homepage: www.cell.com/heliyon

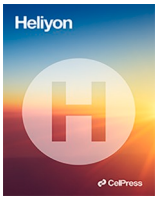

Research article

An experimental toolbox for the physical characterization of thermal insulating polymeric foams

S. Shrestha [a,**], Z. Demchuk [b], F. Polo-Garzon [b], A. Tamraparni [a], J. Damron [b], D. Howard [a], T. Saito [b], A.P. Sokolov [b], D. Hun [a], C. Gainaru [b,*]

[a] Buildings and Transportation Science Division, Oak Ridge National Laboratory, Oak Ridge, TN, 37831, USA
[b] Chemical Sciences Division, Oak Ridge National Laboratory, Oak Ridge, TN, 37831, USA

ARTICLE INFO

Keywords:
Polymeric materials
Closed-cell foams
Optical microscopy
Pycnometry
Dielectric spectroscopy
Thermogravimetric analysis
Mass spectrometry
Nuclear magnetic resonance

ABSTRACT

Recent advancements in polymer science and manufacturing technologies triggered new developments of porous materials used for mitigating heat losses, such as thermal insulating polymeric foams. The major bottleneck in the optimization of these products, however, remains the absence of analytical methods able to scrutinize their large design space reasonably quickly and cost-effectively. This manuscript targets the paucity of data for polymeric foams by illustrating, at a proof-of-principle level, that several well-established analytical methods including optical microscopy, pycnometry, dielectric spectroscopy, thermogravimetric analysis, and nuclear magnetic resonance can be exploited for an extensive, yet logistically efficient, characterization of these materials. The purpose of this study is thus introducing an experimental platform for the characterization of market foam products and for the development of new polymeric foams with pore sizes that are particularly relevant for industrial and residential thermal insulation. Since this work introduces several new methodologies, it may be used as a guide for both laboratory users and specialists in the field, who may further improve the herein proposed experimental concepts.

1. Introduction

The rapid development of porous materials in recent years attests that their specific mechanical, electrical, and thermal properties can be exploited in many technological areas [1,2]. Among these materials, polymeric foams are lightweight, flexible, non-corrosive, and low-cost products employed in a wide range of applications including packaging, food and pharmaceutical industries, advanced manufacturing and, most prominently, thermal insulation [3–7]. In this particular area, intensive efforts are being spent on the deployment of polymer-based building envelopes, currently regarded as one of the most efficient means to minimize global energy consumption for industrial and residential thermal management [8].

Depending on their morphologies, different strategies have been proposed for improving the thermal performance of polymeric foams. In this respect, it is worth noting that foams in general can be of an open- or closed-cell type. The open-cell foams have highly interconnected voids (usually filled with air), whereas the closed-cell ones have pores isolated from each other by matrix walls [9]. Both open- and closed-cell *macro*porous (with pore sizes above 1 μm) polymeric foams are currently used for industrial and residential

* Corresponding author.
** Corresponding author.
E-mail addresses: shresthass@ornl.gov (S. Shrestha), gainarucp@ornl.gov (C. Gainaru).

https://doi.org/10.1016/j.heliyon.2024.e36074
Received 18 April 2024; Received in revised form 21 July 2024; Accepted 8 August 2024
Available online 10 August 2024

thermal insulation on a global scale, having a huge market size [10]. The thermal resistivity of open-cell foams in general is relatively low but can be strongly increased by reducing the dimensions of the pores below the mean free path of their air molecular residents [11–14]. The resulting *micro*porous open-cell foams, with aerogels as a classical example, have relatively high costs and are typically employed in niche applications concerning high thermal insulation of relatively small volumes [15,16]. Regarding closed-cell foams, their thermal resistivity is increased by filling their pores with so-called blowing agents, which are gases with thermal conductivities significantly lower than that of air [17].

The rational development of these porous materials largely relies on feedback-controlled workflows, calling for methodologies able to provide large amounts of information in a relatively short time and at a low cost. The bottleneck, however, is that current techniques for the characterization of polymeric foams are technically challenging, costly, and fairly inaccurate. This situation significantly slows the process of tailoring (i) the morphology and (ii) the composition of these foams toward a progressive increase in their thermal performance [18–21], as discussed next.

Regarding (i) morphological investigations of polymeric foams, their porosities could, in principle, be easily accessed knowing the density of the bulk polymeric matrix (in the absence of pores) and the ratio of their masses and their volumes, the latter with pores included [22]. However, this is not an easy task for foam samples with irregular shapes. In this case, one may attempt estimating their volume via pycnometry, by probing the amount of a purged inert gas that penetrates a certain space that is not occupied by the bulk in which the sample is placed [23–26]. However, since the purged gas will not be able to enter the pores surrounded by matrix walls, this method will not be successful in estimating the porosities of closed-cell foams. Nevertheless, in this specific case the pycnometry technique can still provide valuable information regarding the relative amounts of closed pores, as discussed below in Section III.1.b.

Whereas the estimation of porosity may still be considered a relatively easy task, detailed information regarding pore characteristics requires more elaborate procedures. The most critical parameters in this respect are the average pore size and the pore size distribution. For materials with open pores in the submicron range, the workhorse technique providing this information is gas adsorption [27]. The specific pore size range that can be analyzed with this method depends on several factors, such as the nature of the employed gas, temperature, and pressure, however, it is limited to pore dimensions below 0.3 μm [28]. Beyond this habitat of gas physisorption, for materials with pores in the 1–500 μm range relevant for industrial applications, the current alternatives are mercury intrusion [29] and capillary flow porosimetries [30]. The former requires penetration of mercury in the pores, hence is health hazardous and generally applied for hard materials, such as concrete [31]. The capillary flow method is based on the displacement of a liquid wetting the sample pores by applying a gas under a certain pressure, thus it works only if the pores extend from one side of the sample to the other, as in certain membranes and filters [32]. Considering these limitations, for "regular" thermal insulating polymer foams the most eligible approach to access pore sizes is image processing involving scanning electron microscopy (SEM) [33,34]. The high resolution of this technique is a major advantage, but it comes with several logistical constraints, especially when the number of samples is large. For macroporous polymeric foams, optical microscopy can deliver an amount of relevant information similar to that of its SEM counterpart, with significantly reduced data acquisition time and cost; This will be discussed in Section III.1.a.

In addition, exploiting the contrast between the dielectric proprieties of polymer matrix and pores, the present work introduces the concept of "dielectric porosimetry" [35] as an alternative to mercury intrusion and capillary flow porosimetries. As with these two cases, the dielectric method is applicable for open-cell foams only, however, it is neither destructive nor restricted to pores extending across the sample. Instead, it is well suited for globular-like pores like those found in thermally insulating foams. As will be discussed in Section III.1.c, by relatively simple dielectric spectroscopy-based means, one may access sensitive analytical information regarding the topology of porous materials in a short time and with low experimental costs.

With respect to (ii) *the composition of polymeric foams* designed for thermal insulation (with porosities of about 90%–95 %), the main research focus is on the gas constituents filling the cellular volume and governing the thermal performance of closed-pore materials. In such foams, when they are freshly made, the main pore residents are the blowing agent and some CO_2 formed during the foam fabrication. However, this composition changes during the so-called aging, the process in which the air components migrate into—while the excess CO_2 and gas-blowing agents escape from—the foam [36–38].

To analyze the gas composition in closed pores at a given time, the usual experimental procedure involves two steps [39]. The first, and most laborious one, is the extraction of the gas from the pores. This is usually done by crushing/grinding the foam or by direct sampling using a gas collecting syringe under controlled atmosphere [40]. In a second step, the extracted gas is analyzed using gas chromatography [41,42] and/or mass spectrometry (MS) [43]. Complementing this traditional approach, in the present study we will introduce a *non-destructive* procedure based on nuclear magnetic resonance (NMR) for accessing the amount of blowing agent gas in the foam, even without recourse to calibration standards (Section III.2.b).

In addition, we employed thermogravimetric analysis (TGA) [44], as a standalone method and in combination with MS [45], to trace the fingerprints of the blowing agent (Opteon) being released during the temperature-induced degradation of polyisocyanurate (PIR) foams (Section III.2.a). Our results indicate that the TGA method can provide valuable information regarding the amount of blowing agent incorporated in the closed pores of polymeric foams [42,46].

All in all, the goal of this manuscript is to illustrate that several experimental techniques regularly employed for characterizing bulk polymers can be also adopted to access important physical information on the morphology and composition of macroporous polymeric foams for thermal insulation. The proposed experimental portfolio includes optical microscopy, pycnometry, dielectric spectroscopy, TGA, and NMR. In particular, the newly proposed approaches based on dielectric spectroscopy and NMR could become well-established tools for accessing relevant physical parameters to guide development of the next generation of polymeric foams with improved thermal insulation.

2. Experimental details

2.1. Foam samples

For the present study, we used commercial polyurethane (PUR) as an open-cell foam; as closed-cell foams, we used a commercial PIR with Opteon1100 [47] as the blowing agent and two homemade PIRs (one with and one without this blowing agent). The matrix composition of homemade PIRs included polymethylene diisocyanate, aromatic polyester polyol PS2352 (from Stepan, US), catalysts (potassium octoate, N,N-Dimethylcyclohexylamine), silicone surfactant Tegostab B8513 (from Evonik, US), flame-retardant agent TCPP (from TCC, US), and water.

2.2. Optical microscopy

Optical analysis has been performed using an Olympus BX51 instrument from Microscope Central. The microscope, equipped with a 100 W halogen illumination system, has been used in the transmission mode. The images have been recorded using an AmScope 4K HD Multi-Output camera and analyzed using the AmScope camera software.

2.3. Pycnometry

The relative amount of closed pores has been estimated using a AccuPyc II 1340 pycnometer from Micrometrics. The samples were sealed in the instrument sample chamber of fixed volume (~110 cm^3); nitrogen gas was admitted to the chamber as the displacement medium and then was released into a second chamber for volume measurement [24].

2.4. Dielectric spectroscopy

The dielectric measurements covering a frequency range between 1 and 10^5 Hz were performed using a modular equipment from Novocontrol Technologies including an Alpha-A analyzer connected to a ZGS4 test interface. The investigated PUR foam was cut as a disk with a diameter of 18 cm and a thickness of 2 cm, and it was fully submerged for 10 min in a solution of 0.1 g NaCl salt in 100 g water. Gentle mechanical pressing was employed for the removal of visible air bubbles. The sample was then placed in an invar/sapphire cell which was inserted into a cryostat from Novocontrol Technologies. The latter allowed a temperature stability of 0.2 K, achieved using a Quatro controller. Prior to foam investigation, for reference purposes, another measurement was performed using the dielectric cell filled only with ionic solution (in the absence of foam).

2.5. Thermogravimetric analysis and mass spectrometry

A first set of TGA experiments was conducted to determine the thermal stability of the foams using a TGA Q50 (TA Instruments). For these tests, 10–20 mg of PIR sample were placed on a platinum pan, and the measurements were conducted in the range of temperatures from 20 °C to 800 °C with a 10 °C/min heating rate under nitrogen atmosphere. Additional analysis was conducted using a TGA Q5000 (TA instruments) system coupled with a ThermoStar Pfeiffer mass spectrometer. During these tests, the sample was exposed to synthetic air (20 mL/min). The sample was initially held at ~42 °C for 30 min, then the temperature was ramped up by 10 °C/min until it reached 750 °C. Relevant signals were monitored with the mass spectrometer during this analysis. The time lag between the TGA exhaust gas entering the MS probe (at a single mass-to-charge ratio) and its analysis is about 20 s.

2.6. Nuclear magnetic resonance

The ^1H NMR investigations were performed on a Bruker Avance III 400 MHz spectrometer using a simple single pulse experiment under static conditions, with a 90° pulse of 12 μs and a dead time of 6.4 μs We note that this will systematically underrepresent the most rigid proton phase due to the relatively weak pulse and decay during the dead time. However, this is not a concern for systematic comparisons with the same samples and monitoring of the adsorbed gaseous phase. The ^{19}F experiments were performed on the same system using 90° pulses of 15 μs The receiver gain and the number of scans were kept consistent to facilitate comparison. Solution state experiments were performed on a Bruker NeoBay console at 400 MHz.

3. Results and discussion

3.1. III.1 morphological investigations

a) Optical microscopy

The structural investigations of polymeric foams (with atomic constituents of relatively low atomic numbers) are mostly performed using SEM [33,34], whereas x-ray computing tomography (CT) may be another option for porous matrixes comprising heavy atoms [48,49]. The high resolution of these methods is clearly a major advantage that also comes with several logistics constraints.

In this respect, basic optical microscopy can be a viable alternative for morphological investigations of polymeric foams with pores

in the range of a few to several hundred micrometers as typically used in industrial and residential applications. This is particularly relevant when the number of investigated specimens is large. In such a case, sample preparation and image acquisition are significantly less laborious and can be performed by users with elementary microscopy knowledge.

As Fig. 1 illustrates, for "regular" thermally insulating foams, the relevant morphological insights gained from optical studies are practically the same as the ones obtained with SEM. This figure presents optical images obtained for the homemade PIR sample. These were recorded using the "negative" filter of the camera software, in the absence of any numerical sharpening or smoothing procedures. The following information was gained from a simple visual inspection of these images: The pore sizes vary between 50 and 200 μm, the average wall thickness is about 5 μm, and cell units have four to six struts. These dimensions and quantities, together with the porosity, are highly relevant for the theoretical approaches aiming to estimate the effective gas diffusivities [50–52] and the amount of radiative thermal conductivity of polymeric foams [53]. In addition, these images reveal the presence of interconnected pores whose presence may affect the estimation of their relative amount of closed and open pores, as discussed in the next section.

This example demonstrates that for the study of *meso- and macroporous* polymeric foams, optical microscopy is a feasible alternative to its scanning electron counterpart, providing detailed morphological information in a relatively short time and at a low cost. However, this optical method if not applicable for submicron investigations *e.g.*, for the study of aerogels or for accessing hierarchical structure in cell walls, which require SEM observations.

b) Pycnometry

Gas pycnometry is an analytical technique which is mainly employed to probe the densities of samples with irregular shape, such as powders, ceramics and slurries. To this end, this method uses the displacement of inert gases, such as helium or nitrogen, to measure the volume occupied by a given material [23–26]. In the case of open-cell polymer foams, the corresponding probed volume (which cannot be penetrated by the inert gas) is that of the polymeric matrix, V_{pol}. Using this quantity and knowing the mass of the foam sample m_{pol}, one can estimate the density of the polymer matrix $\rho_{pol} = m_{pol}/V_{pol}$. Whereas for some foams the latter may be also found in the literature, for others with more complex composition (*e.g.*, open-cell PIR) this may not be the case, and pycnometry can be used for tackling this problem.

Knowing the *total* volume (with pores) of the foam sample V_{foam}, one can calculate the effective density of the foam as $\rho_{foam} = m/V_{foam}$. Using the polymer and the foam density one can further estimate the foam porosity as

$$\phi \equiv \frac{\rho_{pol} - \rho_{foam}}{\rho_{pol}}. \tag{1}$$

For closed-cell foams, the situation is more complex because the volume probed by the pycnometer V_{meas} represents the sum of the volumes occupied by the polymer matrix V_{pol} and by the closed pores (V_{closed}), which also cannot be penetrated by the purged gas:

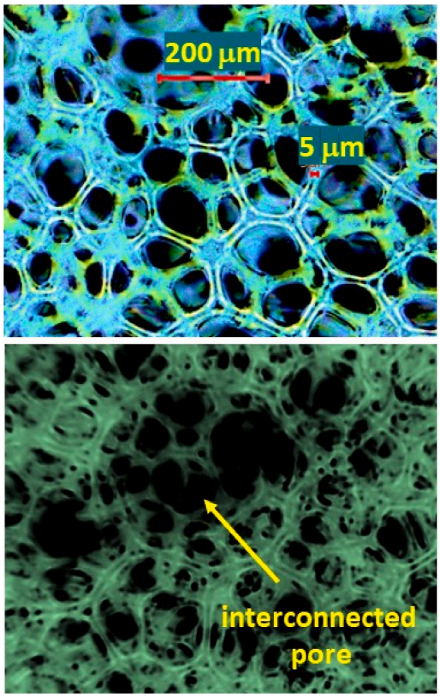

Fig. 1. Optical microscopy images revealing the average pore size, wall thickness, number of struts per cell, and presence of interconnected pores for a homemade PIR foam. These images, obtained in transmission mode, are presented using a negative filter.

$$V_{meas} = V_{pol} + V_{closed}. \tag{2}$$

Instead, for this type of foams, pycnometry can be exploited to estimate the relative amount of closed cells relative to the total number of pores,

$$k \equiv \frac{V_{closed}}{V_{closed} + V_{open}} \tag{3}$$

which practically is always smaller than 100 %. To this end, one combines in Eq. (3) the following expressions for the volumes occupied by the closed cells:

$$V_{closed} = V_{meas} - m/\rho_{pol}, \tag{4}$$

and by the open cells:

$$V_{open} = V_{sample} - V_{meas}. \tag{5}$$

We note that the experimentally accessed V_{closed} may not strictly reflect the sum of the volumes occupied by the elementary closed cells but also that of interconnected open pores, which may also exist in the foam (Fig. 1). If the amount of interconnected pores is significantly large, the relative amount of closed cells may be overestimated.

To provide an example on how pycnometry can be applied for the study of closed-cell foams, in the following we will present the results obtained for the PIR homemade material. The foam was prepared as a cylindrical sample with a diameter of 45 mm and a height of 35 mm. The corresponding weight of this sample was 2.5 g and, considering the sample volume, ρ_{foam} was estimated to be 0.045 g/cm^3. Using a variation between 1.1 and 1.5 g/cm^3 for ρ_{pol}, the porosity of the PIR sample was determined according to Eq. (1) to be $\phi \sim$ 95 %–97 %.

The measurements performed with our pycnometer for 10 cycles at an average temperature of 24 °C using a Nitrogen equilibration rate of 0.005 psi/min indicated an average value for V_{meas} of 49.5 ± 0.1 cm^3. Using the same variation for ρ_{pol} and introducing the above estimations in Eqs. (3)–(5) we obtained a relative amount of close cells $k \sim$ 88 %–90 %. The high values of porosity and of relative number of closed cells, corroborated with the microscopy results revealing relatively large pores and thin pore walls, indicate that the studied PIR foam has a structural morphology well suited for thermal insulation purposes.

We would like to emphasize that the pycnometry investigations of polymeric foams ideally should be performed on samples with relatively large volumes, close to that of the entire analyzer chamber volume. This precludes several experimental pitfalls that can compromise the quality and interpretation of pycnometry data, especially when the focus is on polymeric foams with relatively large pores. For example, large sizes in general reduce the uncertainties in the determination of $V_{foam.}$ For open-cell systems, the use of a large sample can mitigate the errors caused by small ratios between the measured volume V_{meas} and the volume of the pycnometer

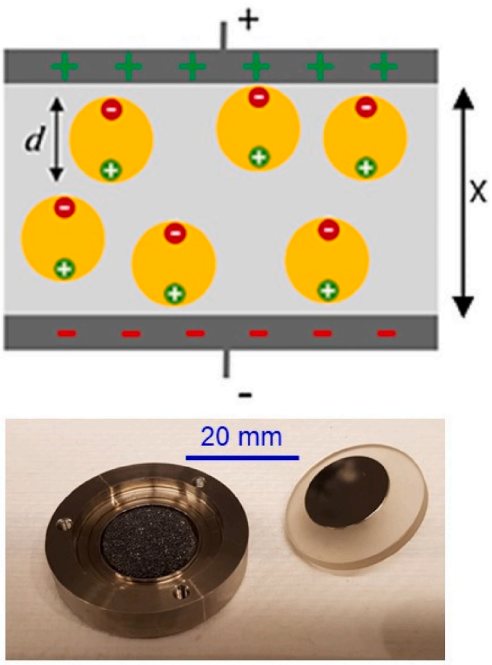

Fig. 2. Schematics of the concept for the estimation of pore sizes using dielectric spectroscopy (top) and the employed dielectric cell filled with the PUR sample (bottom).

chamber. Regarding closed-cell foams, a sizable sample additionally reduces the relative amount of closed pores, which are artificially "opened" during sample cutting. Corrections for such cells' alterations follow ASTM method D-6226-15[54] and are implemented in modern pycnometer software packages. For the homemade PIR sample with geometric parameters provided above, the corresponding correction factor was below 1 %.

c) Dielectric porosimetry

In this section we will introduce an analytical approach for accessing morphological details of polymeric foams based on dielectric spectroscopy. This analytical method is widely employed for the characterization of (bulk) polymers in general, and it relies on the ability of these materials to build up a macroscopic polarization under the influence of electric fields [55]. The dielectric response of heterogeneous polymeric materials has been studied for highly polar domains (with a large dielectric constant) embedded in less polar matrixes [56]. However, to the best of our knowledge, this technique has never been used for the estimation of pore sizes in polymeric foams.

Exploiting this polarity contrast we propose the following dielectric concept for accessing structural information of open-cell foams. To access the sizes of the pores, the foam will be filled with a liquid (*e.g.*, water) containing a small amount of ions (from regular salts), then transferred into a dielectric cell. When the polarity of the dielectric capacitor is changed, the distance that ions are allowed to travel though the liquid will correspond to the effective size of the pores *d*, as schematically illustrated in Fig. 2.

The corresponding ion displacement can be estimated from the experimentally determined frequency (or rate) ν^* representing the inverse of the characteristic time in which the ions migrate from one side of the pore to the other. This frequency is given by the relation

$$\nu * = \frac{1}{2\pi\tau} = \frac{v_D}{2\pi d}, \tag{6}$$

with v_D the drift velocity of ions in the liquid. Additionally, in a reference experiment, one may probe the dielectric response of the cell fully filled with the ionic solution. By these means one can estimate the characteristic frequency $\nu_R{}^*$ corresponding to the motion of ions from one electrode to the other, over the distance x (Fig. 2 top) as $\nu_R{}^* = v_D/(2\pi x)$. Combining this relation with Eq. (6) one can eliminate v_D and extract the effective pore size using the two experimentally probed characteristic frequencies and knowing the reference distance between the electrodes x, according to

$$d = x\frac{\nu_R^*}{\nu^*}. \tag{7}$$

To test the applicability of the proposed approach, in the following we will focus on the dielectric response of a open-cell PUR foam sample for which the scanning electron microscopy information is available [52]. The dielectric spectrum measured at room temperature for PUR soaked in NaCl water solution is shown in the left frame of Fig. 3(a). The response plotted in terms of tangent of the loss angle (tanδ) as a function of frequency displays a maximum, and its position was used for the identification of the characteristic frequency ν^* of about 6×10^3 Hz. With the geometrical parameter x (~50 μm) and the reference characteristic frequency $\nu_R{}^*$ of about

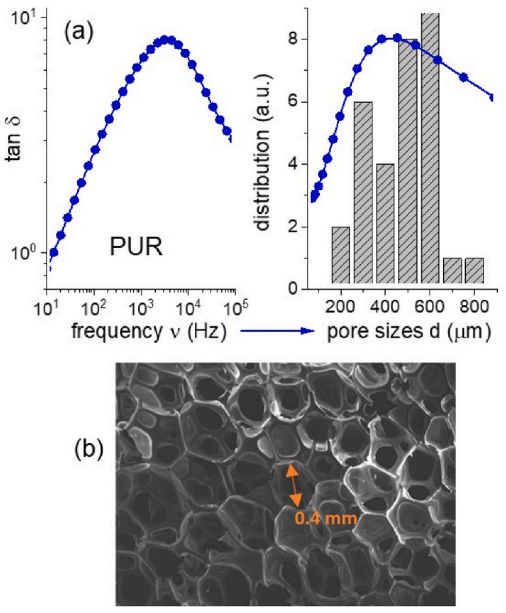

Fig. 3. (a) Dielectric spectrum of polyurethane foam, its conversion to pore size distribution, and (b) the electron microscopy scan of the same material. The right frame of (a) includes the pore size distribution as obtained from the analysis of the image included in (b) using ImageJ software.

5×10^4 Hz determined from for the investigation of the ionic solution alone, one has now all necessary information for extracting the mean pore size d according to Eq. (7).

However, since the dielectric signal is probed in a broad frequency range, one may go one step further in the analysis. One can note from the non-Lorentzian shape of this dielectric response (Fig. 3(a), left) that the material is characterized not by a single, but by a distribution of characteristic frequencies that reflect an underlying distribution of pore sizes. Therefore, using the same Eq. (7), the x-scale of Fig. 3(a) left can be converted from frequency to pore sizes, as shown in Fig. 3(a) right. Nevertheless, the main information accessed in this proof-of-principle test is that the pore sizes for this particular polyurethane sample are centered around 400–500 μm.

For comparison, the right frame of Fig. 3(a) includes the pore side distribution determined from the analysis of the SEM scan using the ImageJ software. In addition, Figure A1 in the Appendix presents a similar dielectric/SEM analysis performed for another type of foam, namely high-density polystyrene (HDPS). For the latter the relevant pore sizes are distributed around 30 μm. Nevertheless, in both cases the dielectric distributions appear to cover the relevant pore size ranges, although some differences can be noticed for the PUR case. In this regard, one should note that the dielectrically probed distribution reflects practically all the pores in the studied volume, while image analyses a significantly smaller number of pores (about 30) located near the cut surface.

We note that the present idea has been conceived based on our previous experience with ionic transport within limited boundaries, which gives rise to the so-called Maxwell-Wagner [57] and electrode polarization effects [58]. These phenomena occur when the transport of charge carriers is impeded by structural heterogeneities in the bulk or by the probing electrodes. Such finite-size induced polarization processes occurs if the diffusion path of ions is larger than their screening (Debye) length [55]. For example, a solution of NaCl in water at 25 °C and a concentration of 10-3 M has a Debye length of about 10 nm, but for water itself (with protons as charge carriers) this length is about 100 nm. In our view, this method will not be applicable for pores below 1 μm.

Therefore, the success of the herein proposed "dielectric porosimetry" relies, to a certain degree, on the relatively large size of the pores, which also favors the penetrations of the aqueous solution in the foam. However, for large pores, the volume of the investigated sample should also be large, so that the number of pores remains statistically relevant. Other limitations of this approach are that it is not applicable for electrically conducting (*e.g.*, metallic) foams and that water may not wet all types of porous materials because some of them may be hydrophobic. To tackle the latter issue, which is also a concern for capillary flow porosimetry [30], one may choose another liquid as the ionic matrix. Low-viscous liquids in general have their own dielectric absorption processes in the GHz frequency range, hence their response will not overlap with the much slower one corresponding to the migration of ions within macropores.

Regarding logistics, the acquisition time of the dielectric spectrum is about 5 min, which renders the overall time for the investigation of one sample to less than 1 h. Considering the simplicity in sample preparation, data acquisition, and analysis, the above results suggests that the proposed dielectric approach has the potential to become a well-established analytical tool for accessing the size of open pores in polymeric foams.

3.2. III.2 accessing the amount of blowing agent

In general, the thermal insulating characteristics of closed-cell polymeric foams are considerably superior to those of their open-cell counterparts. This is because the thermal conductivity of blowing agent gasses is significantly lower than that of air. In this regard, estimating the amount of blowing agents which is actually trapped in the pores is important, considering that in the strongly exothermic process of foam formation a relevant percentage of their initial amount may be lost. Therefore, in this work we will introduce a novel, non-destructive method to access the amount of blowing agent gases in the pores using NMR.

Before this, however, we note that a recent study reported, based on results obtained with the solvent extraction method, "30 % of the blowing gas was found in the condensed form" in foams containing cyclopentane as a blowing agent [42]. This made us wonder

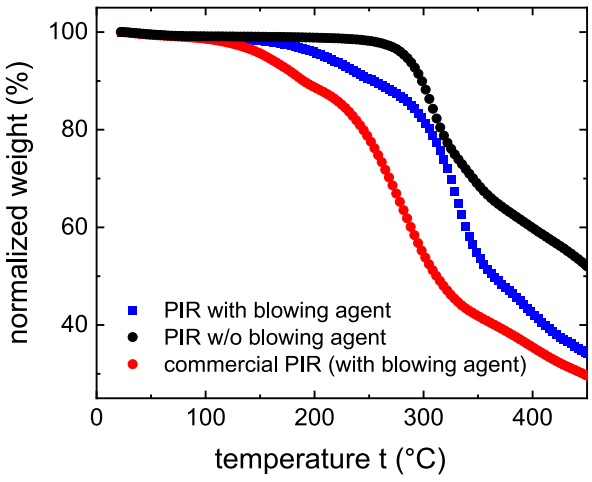

Fig. 4. Thermogravimetric response of commercial PIR and two homemade PIR foams, one containing Opteon and the other lacking a blowing agent in its composition, from first experiments.

how general this observation is, and whether a similar situation—with Opteon being partially incorporated in the condensed form in the matrix in addition to the gas state in the pores—could also occur for our PIR foams. To address this point we employed thermogravimetric investigations, as discussed next.

a) Thermogravimetric analysis

TGA is an analytical method in which variation in the mass of a sample is measured with high accuracy as a function of ramping temperature. This type of measurement is usually employed to provide information on adsorption/desorption phenomena, quality control of newly synthesized materials (by tracing the amount of water and/or solvents), and accessing the decomposition temperature of chemical products [44,59].

With this technique in our laboratory portfolio, we initially employed it to check the influence of high temperatures on the structural integrity of PIR foams. For these tests we used the commercial PIR with Opteon and two homemade PIR foams, one with and the other devoid of this blowing agent. The relative changes in the weight of these materials occurring upon increasing temperature are plotted in Fig. 4. As observed here, all samples display a small change in their mass as the temperature is increased to about 100 °C, assigned to the presence of moisture in their initial state. As the temperature is further increased to about 350°C-400 °C, the two PIR samples containing blowing agents exhibit two stages of weight decay, whereas the foam lacking Opteon in its composition exhibits only one stage.

To gain additional information on this intriguing phenomenology, we performed a second set of experiments on the two PIR samples with and without a blowing agent using a different TGA instrument with the gas exhaust connected to an MS analyzer. Before these tests, we recorded the MS spectrum of Opteon to identify its characteristic mass-to-charge ratio ($m/z \sim 95$ amu). The evolution of the MS signal accordingly tunned for Opteon was monitored while the temperature of the two foams was continuously increased in the TGA oven. The corresponding results are shown in Fig. 5, with (a) presenting the evolution in relative weight and (b) showing the evolution of the MS intensity corresponding to Opteon.

As observed in the figure, the MS measurements of the PIR devoid of blowing agent display only background noise. For the PIR foam with the blowing agent, however, the MS intensity increases above 100 °C and reaches a maximum intensity followed by a sharp decrease at temperatures similar to those at which the first weight decay is completed (see vertical dashed line in Fig. 5). These results indicate that the first TGA decay step leads to the release of Opteon.

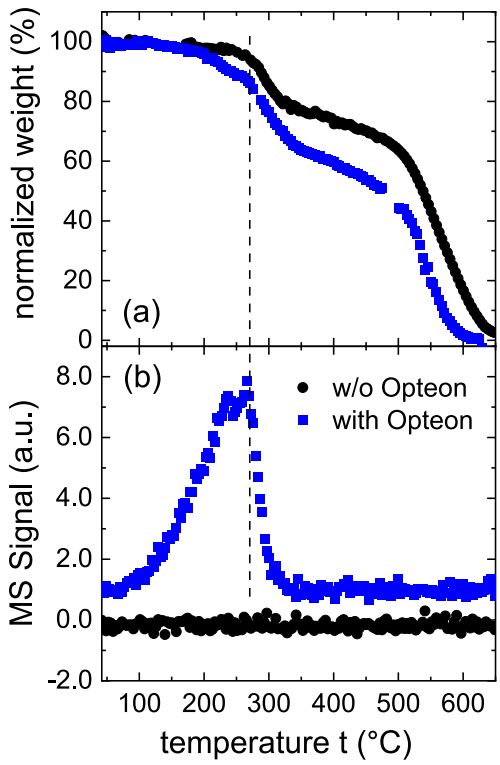

Fig. 5. (a) TGA responses probed in the second set of experiments for the two homemade PIR foams, one containing Opteon and the other lacking this blowing agent in its composition. (b) The corresponding Opteon MS signals probed at a constant mass-to-charge ratio m/z of 95 amu, see text for details.

Since the present MS investigation cannot provide information on the total amount of Opteon being recorded, the question remains whether before the thermal degradation this blowing agent has been trapped in the foam as a gas in the pores, or in a condensed state inside the polymer matrix. The NMR results discussed next indicate that for our homemade PIR foam the first scenario prevails.

b) Nuclear magnetic resonance

Owing to its advantage of high isotope selectivity, NMR is often employed to nondestructively access the composition and local dynamics of various materials [60]. Its applicability becomes particularly relevant when the structural constituents contain nuclear species with high sensitivity to external magnetic fields and different Larmor frequencies [61]. At natural isotopic abundance, ^{1}H and ^{19}F are the most suitable nuclei for NMR studies, opening the venue for morphological and dynamical investigations for a wide range of materials containing these species.

Based on these considerations, we tested whether this technique can be employed to provide information regarding the amount of blowing agents in polymeric foams. For this purpose, we have chosen our PIR sample containing Opteon, which incorporates in its molecular structure both ^{1}H and ^{19}F nuclei (inset of Fig. 6[a]). The corresponding sample was prepared by pushing a cylindrical piece of a freshly made foam in the NMR tube to fill its bottom part. The ^{1}H and ^{19}F spectra were collected at room temperature.

Focusing first on the ^{19}F results, these are presented in Fig. 6(a). Considering that the polymer matrix does not contain fluorine atoms, the clear presence of an NMR line indicates that the sensitivity of this method is good enough to reveal the presence of Opteon. Because the line appears as relatively sharp, the corresponding ^{19}F nuclei are in the fast-motion limit, hence in the gas phase. This implies that NMR can indeed detect the presence of the blowing agent in the pores of PIR foam. To quantify the absolute amount of Opteon in the slice of the sample probed in the NMR experiment, one has the option to measure in a different experiment the corresponding response of this gas at a known pressure (which can be converted to molar concentration using the ideal gas law), then compare the areas of the two corresponding ^{19}F lines. However, if the focus is on the effective diffusivity of this blowing agent in aging investigations [38,41], then one may monitor, eventually at different temperatures, the relative change in the intensity of the ^{19}F NMR signal as a function of time.

Although accessing absolute amounts of gas blowing agents based on ^{19}F NMR is not straightforward, the ^{1}H response may be manipulated to provide such information without recourse to external standards. The proton spectrum of the same PIR foam, recorded under exactly the same experimental conditions as in the fluorine case, is shown in Fig. 6(b). Here one recognizes that the NMR response is more complex, comprising in addition to a sharp line another broad feature in the background. According to the literature, ^{1}H NMR is well suited to quantify phase contrast, particularly for changes of state where molecular mobility differences are extreme [61,62]. As in the ^{19}F case, the narrow feature corresponds to the fast-moving protons in the gas phase; considering that the sample was freshly made these protons can be attributed to Opteon. Pointing to the same conclusion is that the peak position of ~8.6 ppm is

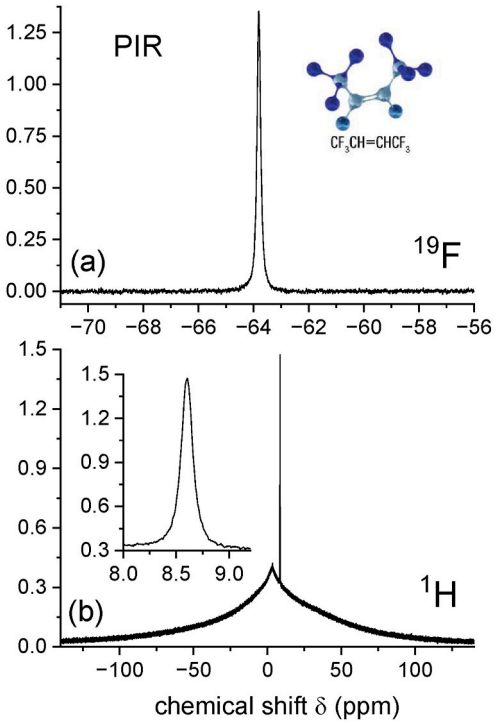

Fig. 6. (a) Fluorine and (b) proton NMR spectra of a PIR foam sample containing Opteon as a blowing agent. The insets present in (a) the chemical structure of Opteon and in (b) a zoom of the sharp line corresponding to fast-moving protons.

consistent with the presence of alkenes and is far from that of residual water, ~5 ppm [63]. Thus, proton NMR can also be used to nondestructively investigate the kinetics of the release process of a blowing agent from these foams, as discussed previously for ^{19}F. This reveals the prospect of employing this method to the investigation of a wide range of foams with different blowing agents, as most of them contain protons.

The second, broad feature with relatively lower intensity in Fig. 6(b) arises from the presence of protons in the quasistatic limit, hence in the condensed state, where substantial $^{1}H/^{1}H$ dipolar broadening is not averaged by fast molecular motion. The presence of this two-phase spectrum can be exploited for extracting the relative amount of protons in the gas phase, and implicitly the amount of the blowing agent in the pores. This can be done by analyzing the ratio of the two areas corresponding to fast (inset of Fig. 6(b)) and slow NMR components, knowing the number density of protons in the immobile polymer matrix. Because the exact composition of the investigated foam cannot be disclosed in this work, we will only mention that the relative amount of Opteon *gas* estimated with this approach corresponds to about 8 % from the total mass of the foam.

This relative weight is in good agreement with the magnitude of the first TGA step (Figs. 4 and 5a) and also corresponds to that used in the recipe of the foam precursor. Based on this comparison, we can conclude that after the foam production, most of the incipient blowing agent is located as gas in the pores, at variance with the situation reported for foams containing cyclopentane in Ref. [42].

To our knowledge, such NMR analysis providing direct estimation of the amount of blowing agent in the pores has not been previously introduced in the literature. In our view, this is yet another analytical approach that can be adopted to gain valuable insights, in a non-destructive manner, on the composition of thermally insulating foams.

4. Conclusions

The present work describes an experimental platform for a multifaceted investigation of polymeric foams for thermal insulation. This includes optical microscopy, pycnometry, dielectric spectroscopy, thermogravimetric analysis, and nuclear magnetic resonance, methods found in most characterization laboratories. The presented data for macroscopic porous foams demonstrate that (i) optical microscopy can deliver the same amount of morphological information as its SEM counterpart, (ii) pycnometry can be exploited to provide the relative amount of closed cells, (iii) dielectric spectroscopy can access the mean pore size and the pore size distribution in open-cell foams, (iv) thermogravimetric analysis can access the amount of blowing agent, and (v) nuclear magnetic resonance can nondestructively deliver information on the amount of the latter as gas in the pores. The herein proposed analytical approach paves the way for a deeper understanding of the physical mechanisms governing the thermal insulation of polymeric foams and facilitates the expedited design of novel porous products optimized for low-carbon-footprint thermal management.

CRediT authorship contribution statement

S. Shrestha: Writing – review & editing, Project administration, Funding acquisition, Conceptualization. **Z. Demchuk:** Writing – review & editing, Methodology, Investigation. **F. Polo-Garzon:** Writing – review & editing, Methodology, Investigation. **A. Tamraparni:** Writing – review & editing, Methodology, Investigation. **J. Damron:** Writing – review & editing, Methodology, Investigation. **D. Howard:** Writing – review & editing. **T. Saito:** Writing – review & editing, Project administration, Funding acquisition. **A.P. Sokolov:** Writing – review & editing, Methodology. **D. Hun:** Writing – review & editing, Funding acquisition. **C. Gainaru:** Writing – review & editing, Writing – original draft, Supervision, Methodology, Investigation, Conceptualization.

Declaration of competing interest

The authors declare the following financial interests/personal relationships which may be considered as potential competing interests:

Catalin Gainaru reports financial support was provided by US Department of Energy. S. Shrestha reports financial support was provided by US Department of Energy. A. Tamraparni reports financial support was provided by US Department of Energy. D. Howard reports financial support was provided by US Department of Energy. T. Saito reports financial support was provided by US Department of Energy. D. Hun reports financial support was provided by US Department of Energy. If there are other authors, they declare that they have no known competing financial interests or personal relationships that could have appeared to influence the work reported in this paper.

Acknowledgement

This work is supported by the projects “Multi-Scale Simulations and Machine Learning-Guided Design and Synthesis of High-Performance Thermal Insulation Materials” and “Barrier Facers for Aged Foam Boards with >R8/in” funded by the Builśding Technologies Office, Office of Energy Efficiency & Renewable Energy at the US Department of Energy.

Appendix

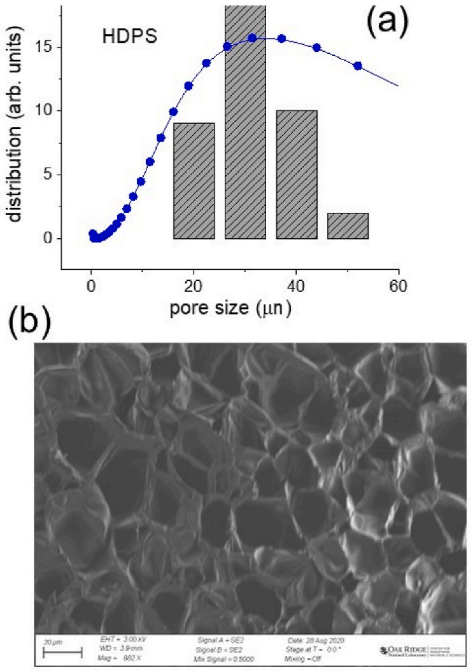

Fig. A1. (a) Dielectrically accessed pore size distribution, and (b) the electron microscopy scan of a high-density polystyrene (HDPS) foam. Frame (a) includes the pore size distribution obtained from the analysis of the image included in (b) using ImageJ software.

References

[1] S. Das, P. Heasman, T. Ben, S. Qiu, Porous organic materials: strategic design and structure–function correlation, Chem. Rev. 117 (2017) 1515.
[2] A. Thomas, Much ado about nothing—a decade of porous materials research, Nat. Commun. 11 (2020) 4985.
[3] L. Li, D. Xu, S. Bai, N. Chen, Q. Wang, Progress in preparation of high-performance and multi-functional polymer foams, Polym. Sci. 1–15 (2023).
[4] M.S. Al-Homoud, Performance characteristics and practical applications of common building thermal insulation materials, Build. Environ. 40 (2005) 353.
[5] B.P. Jelle, A. Gustavsen, R. Baetens, The path to the high performance thermal building insulation materials and solutions of tomorrow, J. Build. Phys. 34 (2010) 99.
[6] A.M. Papadopoulos, E. Giama, Environmental performance evaluation of thermal insulation materials and its impact on the building, Build. Environ. 42 (2007) 2178.
[7] G.M. Zaki, A.M. Al-Turki, Optimization of multilayer thermal insulation for pipelines, Heat Tran. Eng. 21 (2000) 63.
[8] AR5 Climate Change, Mitigation of climate change — IPCC. https://www.ipcc.ch/report/ar5/wg3//, 2014.
[9] L. Pilon, A.G. Fedorov, R. Viskanta, Gas diffusion in closed-cell foams, J. Cell. Plast. 36 (6) (2000) 451–474.
[10] US Energy Information Administration, Annual Energy Outlook 2021, 2021. Washington, DC.
[11] S.S. Kistler, The relation between heat conductivity and structure in silica aerogel, J. Phys. Chem. 39 (1) (1935) 79–85.
[12] H.F. Gangåssæter, B.P. Jelle, S.A. Mofid, T. Gao, Air-filled nanopore based high-performance thermal insulation materials, in: Energy Procedia, vol. 132, Elsevier Ltd., 2017, pp. 231–236.
[13] G.H. Tang, C. Bi, Y. Zhao, W.Q. Tao, Thermal transport in nano-porous insulation of aerogel: factors, models and outlook, Energy 90 (2015) 701–721.
[14] T. Feng, J. He, A. Rai, D. Hun, J. Liu, S.S. Shrestha, Size effects in the thermal conductivity of amorphous polymers, Phys. Rev. Appl. 14 (2020) 044023.
[15] C. Jin, Aerogels super-thermal insulation materials by nano hi-tech, in: Aerogels Handbook, Springer, New York, 2011, pp. 865–877.
[16] H. Yu, H. Zhang, J. Zhao, et al., Thermal conductivity of micro/nano-porous polymers: prediction models and applications, Front. Physiol. 17 (2022) 23202.
[17] W. Zhai, J. Junjie, C.B. Park, A review on physical foaming of thermoplastic and vulcanized elastomers, Polym. Rev. 62 (2022) 95.
[18] Z. Wang, C. Ma, C. Zhang, X. Li, S. Duan, M. Chen, Study on all water foaming of rigid polyurethane foam and design of high-performance formula, in: IOP Conference Series: Earth and Environmental Science, vol. 446, Institute of Physics Publishing, 2020.
[19] J. Peyrton, L. Avérous, Structure-properties relationships of cellular materials from biobased polyurethane foams. Materials Science and Engineering R: Reports, Elsevier Ltd, July 1, 2021.
[20] P. Kosmela, A. Hejna, J. Suchorzewski, Ł. Piszczyk, J.T. Haponiuk, Study on the structure-property dependences of rigid PUR-PIR foams obtained from marine biomass-based biopolyol, Materials 13 (5) (2020).
[21] Q. Xu, T. Hong, Z. Zhou, J. Gao, L, The effect of the trimerization catalyst on the thermal stability and the fire performance of the polyisocyanurate-polyurethane foam, Fire Mater. 42 (1) (2018) 119–127.
[22] F. M. de Souza, Y. Desai, and R. K. Gupta, Introduction to polymeric foams in polymeric foams: fundamentals and types of foams (volume 1), ACS (Am. Chem. Soc.) Symp. Ser. Vol. 1439, Chapter 1, pp 1–23.
[23] H.G.T. Nguyen, et al., Understanding material characteristics through signature traits from Helium Pycnometry, Langmuir 35 (2019) 2115.

[24] M. Viana, P. Jouannin, C. Pontier, D. Chulia, About pycnometric density measurements, Talanta 57 (3) (2002) 583–593.
[25] J. Engstrand Unosson, C. Persson, H. Engqvist, An evaluation of methods to determine the porosity of calcium phosphate cements, J. Biomed. Mater. Res. B Appl. Biomater. 103 (1) (2015) 62–71.
[26] A. Amoozegar, J.L. Heitman, C.N. Kranz, Comparison of soil particle density determined by a gas pycnometer using helium, nitrogen, and air, Soil Sci. Soc. Am. J. 87 (1) (2023) 1–12.
[27] S. Scaife, P. Kluson, N. Quirke, Characterization of porous materials by gas adsorption: do different molecular probes give different pore structures? J. Phys. Chem. B 104 (2000) 313.
[28] A. Orsikowsky-Sanchez, C. Franke, A. Sachse, E. Ferrage, S. Petit, J. Brunet, F. Plantier, C. Miqueu, Gas porosimetry by gas adsorption as an efficient tool for the assessment of the shaping effect in commercial zeolites, Nanomaterials 11 (5) (2021 May 1) 1205.
[29] A.B. Abell, K.L. Willis, D.A. Lange, Mercury intrusion porosimetry and image analysis of cement-based materials, J. Colloid Interface Sci. 211 (1999) 39.
[30] W.R. Wise, A new insight on pore structure and permeability, Water Resour. Res. 28 (1992) 189.
[31] A.B. Abell, K.L. Willis, D.A. Lange, Mercury intrusion porosimetry and image analysis of cement-based materials, J. Colloid Interface Sci. 211 (1) (1999) 39–44.
[32] H.E. Kolb, R. Schmitt, A. Dittler, G. Kasper, On the accuracy of capillary flow porometry for fibrous filter media, Separ. Purif. Technol. 199 (2018) 198–205.
[33] R. Jahanmardi, B. Kangarlou, A.R. Dibazar, Effects of organically modified nanoclay on cellular morphology, tensile properties, and dimensional stability of flexible polyurethane foams, J Nanostruct. Chem. 3 (2013) 82.
[34] S. Flores-Bonano, J. Vargas-Martinez, O.M. Suárez, W. Silva-Araya, Tortuosity index based on dynamic mechanical properties of polyimide foam for aerospace applications, Materials 12 (2019) 1851.
[35] A. Mansuri, P. Münzner, A. Heermant, F. Patzina, T. Feuerbach, J. Winck, A.W.P. Vermeer, W. Hoheisel, R. Böhmer, C. Gainaru, M. Thommes, Characterizing phase separation of amorphous solid dispersions containing imidacloprid, Mol. Pharm. 20 (4) (2023) 2080.
[36] D. Bhattacharjee, J.R. Booth, Effective diffusion coefficients of CO_2 and HCFC-22 in polyurethane and polyisocyanurate foams, J. Cell. Plast. 31 (3) (1995) 244–259.
[37] A. Galakhova, M. Santiago-Calvo, J. Tirado-Mediavilla, F. Villafañe, M.A. Rodríguez-Pérez, G. Riess, Identification and quantification of cell gas evolution in rigid polyurethane foams by novel GCMS methodology, Polymers 11 (7) (2019) 1192.
[38] J. Andersons, J. Modniks, M. Kirpluks, Estimation of the effective diffusivity of blowing agents in closed-cell low-density polyurethane foams based on thermal aging data, J. Build. Eng. 44 (2021) 103365.
[39] H. Macchi-Tejeda, et al., Contribution to the gas chromatographic analysis for both refrigerants composition and cell gas in insulating foams Part I: method, Int. J. Refrig. 30 (2007) 329–337.
[40] A. Galakhova, M. Santiago-Calvo, J. Tirado-Mediavilla, F. Villafañe, M.Á. Rodríguez-Pérez, G. Riess, Identification and quantification of cell gas evolution in rigid polyurethane foams by novel GCMS methodology, Polymers 11 (2019) 1192.
[41] H. Macchi-Tejeda, H. Opatova, J. Guilpart, Contribution to the gas chromatographic analysis for both refrigerants composition and cell gas in insulating foams—Part II: aging of insulating foams, Int. J. Refrig. 30 (2007) 338–344.
[42] U. Berardi, J. Madzarevic, Microstructural analysis and blowing agent concentration in aged polyurethane and polyisocyanurate foams, Appl. Therm. Eng. 164 (2020) 114440.
[43] M. Modesti, A. Lorenzetti, C. Dall'acqua, New experimental method for determination of effective diffusion coefficient of blowing agents in polyurethane foams, Polym. Eng. Sci. 44 (2004) 12.
[44] R. Mansa, S. Zou, Thermogravimetric analysis of microplastics: a mini review, Environmental Advances 5 (2021) 100117. ISSN 2666-7657.
[45] W.M. Jones, J.B. Tapia, R.R. Tuttle, M.M. Reynolds, Thermogravimetric analysis and mass spectrometry allow for determination of chemisorbed reaction products on metal organic frameworks, Langmuir 36 (14) (2020) 3903–3911.
[46] J. Booth, Some factors affecting the long-term thermal insulating performance of extruded polystyrene foams, in: R. Graves, D. Wysocki (Eds.), Insulation Materials: Testing and Applications, vol. 2, ASTM International, West Conshohocken, PA, 1991, pp. 197–213.
[47] https://www.opteon.com/en/products/foam-blowing/1100.
[48] X. Ou, X. Zhang, T. Lowe, R. Blanc, M.N. Rad, Y. Wang, N. Batail, C. Pham, N. Shokri, A.A. Garforth, P.J. Withers, X. Fan, X-ray micro computed tomography characterization of cellular SiC foams for their applications in chemical engineering, Mater. Char. 123 (2017) 20–28.
[49] P.J. Withers, C. Bouman, S. Carmignato, et al., X-ray computed tomography, Nat Rev Methods Primers 1 (2021) 18.
[50] E.F. Cuddihy, J. Moacanin, Diffusion of gases in polymeric foams, J. Cell. Plast. 3 (2) (1967) 73–80, https://doi.org/10.1177/0021955X6700300202.
[51] A.G. Ostrogorsky, L.R. Glicksman, Time variation of insulating properties of closed cell foam insulation, J. Therm. Insul. 12 (4) (1989) 270–283.
[52] S.S. Shrestha, J. Tiwari, A. Rai, D.E. Hun, D. Howard, A.O. Desjarlais, M. Francoeur, T. Feng, Solid and gas thermal conductivity models improvement and validation in various porous insulation materials, Int. J. Therm. Sci. 187 (2023) 108164.
[53] L. Glicksman, M. Schuetz, M. Sinofsky, Radiation heat transfer in foam insulation, Int. J. Heat Mass Tran. 30 (1) (1987) 187–197.
[54] Standard Test Method for Open Cell Content of Rigid Cellular Plastics in Book of Standards Volume: 08.03 Developed by Subcommittee: D20.22, DOI: 10.1520/D6226-15.
[55] F. Kremer, A. Schonhals (Eds.), Broadband Dielectric Spectroscopy, Springer-Verlag, 2002.
[56] R. Richert, Dielectric spectroscopy and dynamics in confinement, Eur. Phys. J. Spec. Top. 189 (2010) 3746.
[57] C. Gainaru, S. Schildmann, R. Böhmer, Surface and confinement effects on the dielectric relaxation of a monohydroxy alcohol, J. Chem. Phys. 135 (17) (2011) 174510.
[58] R. Kumar, et al., A Rayleighian approach for modeling kinetics of ionic transport in polymeric media, J. Chem. Phys. 146 (2017) 064902.
[59] A.W. Coats, J.P. Redfern, Thermogravimetric analysis: a review, Analyst 88 (1053) (1963) 906–924.
[60] K. Schmidt-Rohr, H.W. Spiess, Multidimensional Solid-State NMR and Polymers, Academic Press, London, 1994.
[61] V. Räntzsch, M. Haas, M.B. Özen, K.-F. Ratzsch, K. Riazi, S. Kauffmann-Weiss, J.K. Palacios, A.J. Müller, I. Vittorias, G. Guthausen, M. Wilhelm, Polymer crystallinity and crystallization kinetics via benchtop 1H NMR relaxometry: revisited method, data analysis, and experiments on common polymers, Polymer 145 (2018) 162–173.
[62] M. Balci, in Basic 1H- and 13C-NMR Spectroscopy (first ed., Elsevier).
[63] R.M. Silverstein, G.C. Bassler, T.C. Morrill, Spectrometric Identification of Organic Compounds, fifth ed., Wiley, 1991.